

7-22-2020

## On the Positivity of the Discrete Green's Function for Unstructured Finite Elements Discretizations in Three Dimensions

Andrew Miller

University of Connecticut - Storrs, [andrew.miller@uconn.edu](mailto:andrew.miller@uconn.edu)

Follow this and additional works at: <https://opencommons.uconn.edu/dissertations>

---

### Recommended Citation

Miller, Andrew, "On the Positivity of the Discrete Green's Function for Unstructured Finite Elements Discretizations in Three Dimensions" (2020). *Doctoral Dissertations*. 2582.  
<https://opencommons.uconn.edu/dissertations/2582>

# On the Positivity of the Discrete Green's Function for Unstructured Finite Elements Discretizations in Three Dimensions

Andrew Miller, Ph.D.

University of Connecticut, 2020

## ABSTRACT

The aim of this thesis is twofold. First, we will establish new estimates for the discrete Green's function and obtain some positivity results. In particular, we establish that the discrete Green's functions with singularity in the interior of the domain cannot be bounded uniformly with respect of the mesh parameter  $h$ . Actually, we show that at the singularity the Green's function is of order  $h^{-1}$ , which is consistent with the behavior of the continuous Green's function. In addition, we also show that the discrete Green's function is positive and decays exponentially away from the singularity. We also establish numerically persistent negative values of the discrete Green's function on Delaunay meshes which then implies a discrete Harnack inequality cannot be established for unstructured Finite Element discretizations. Of independent interest we also prove  $L^p$  estimates for a regularized Green's function in three dimensions which may have implications in establishing best approximation results in optimal control.

# On the Positivity of the Discrete Green's Function for Unstructured Finite Elements Discretizations in Three Dimensions

Andrew Miller

M.A. Rhode Island College 2014

B.A. Rhode Island College 2012

A Dissertation

Submitted in Partial Fulfillment of the

Requirements for the Degree of

Doctor of Philosophy

at the

University of Connecticut

2020

Copyright by

Andrew Miller

2020

**APPROVAL PAGE**

Doctor of Philosophy Dissertation

**On the Positivity of the Discrete Green's  
Function for Unstructured Finite Elements  
Discretizations in Three Dimensions**

Presented by

Andrew Miller, B.A., M.A.

Major Advisor

\_\_\_\_\_  
Dr. Dmitriy Leykekhman

Associate Advisor

\_\_\_\_\_  
Dr. Vasileios Chousionis

Associate Advisor

\_\_\_\_\_  
Dr. Jeffrey Connors

University of Connecticut

2020

## ACKNOWLEDGMENTS

First and foremost, I would like to sincerely thank my advisor, Dr. Dmitriy Leykekhman. Words cannot express how grateful I am for his guidance, patience, and ability to remotivate me when my frustration was at its highest. Without Dmitriy's support I do not believe I would become as successful a mathematician as I am today. He also took a genuine interest in my own personal goals. Knowing I wanted a teaching focused position his support balanced between my pursuit of extra teaching opportunities while also pushing me to be a better researcher. Out of my peers, I have never been the strongest mathematically, however, Dmitriy never once made me feel as though I couldn't do it. Dmitriy; thank you for being there for me, I am thankful for our mathematical conversations and all of our one off conversations about some of the most random topics imaginable. You have made me laugh more times than I can count and I am looking forward to continuing to work with you in the time to come.

I would also like to express my thanks to Dr. Vasileios Chousionis and Dr. Jeffrey Connors. During my time at UConn I have taken many courses and have had many conversations with them. Their support of my goals was and is also unwavering. I am grateful that their doors were always open, they also had an excellent ability to revitalize me during times of struggle. In particular, I would like to thank Vasilis for his mentorship since my second semester at UConn.

I owe a lot of my development as an educator to Dr. Amit Savkar. He recognized early on my passion for teaching and consistently challenged and pushed me to improve my

teaching. During the summer of 2019 we worked together on developmental algebra skills for UConn's Student Support Services program. As difficult a task as it was, I learned a great deal from Amit in a short five weeks. In addition, we had many conversations about how to attack the job market, without these I don't believe I would have my position at Bridgewater State. Furthermore, I owe a lot to the opportunities that Dr. Bidya Ranjeet (Student Support Services) and Kevin McLaughlin (BRIDGE Engineering) afforded me in teaching historically underrepresented students. I am looking forward to taking all that I have learned to continually improve supporting all my students.

I am lucky to have met a number of graduate students from various departments across campus. One thing I can say for certain is the support of all mathematics faculty at UConn is unique and special. Everyone from the graduate directors, Dr. Choi, Dr. Yan, and Dr. Solomon, to professors I had in prelim courses, to professor I worked with on teaching assignments. There was not a single person I did not feel comfortable talking to about virtually any issue. There was also never a time where I did not feel as though the faculty had my back. I certainly owe a part of my success to the entire department for their dedication to all graduate students.

I am also grateful for the amazing support staff in the math department: Dr. Gross, Monique Roy, Tammy Prentice, and Rachel D'Antonio. Anything I ever needed was taken care of by the staff. In particular, thank you to Monique. Monique sets the example on campus for her support of graduate students. When looking to escape my work I could always count on Monique to have a conversation about sports, traveling, or even school in general. She would always set time aside for graduate students and we all owe a lot of our successes to her.

I also owe a very special thank you to Dr. Christopher Teixeira at Rhode Island College. Chris was my advisor during my undergrad and he had the foresight to pull me aside during

my sophomore year to set my course straight after initially struggling as a math major. From then on he always pushed me to do more and to be better. Both mathematically and in my teaching. I would have never considered a PhD program if it were not for Chris. As one of my best friends today I can say Chris has changed my life in way that are almost unfathomable. The deeps of my gratitude knows no bounds.

To the many other faculty at RIC who played an integral role in my development as a mathematician and educator I most certainly owe a huge thank you. In particular, Dr. Lisa Humphreys, Dr. Raimundo Kovac, Dr. Stephanie Costa, Dr. David Abrahamson, Dr. Rebecca Sparks, Dr. John Burke and Dr. Vivian Laferla. The support you all gave during and after my time at RIC is incredibly touching and I am fortunate to call you all friends today.

I recall a week during my first semester at UConn, driving to school on route 6 in Willimantic with Kyle Allaire. I had just failed my first mid-term exams in Modern Analysis and Topology. All I could think was, “there is no way I am finishing this program”. I met Kyle during my undergrad in a College Geometry course and we have worked side by side ever since. Without his support throughout my five years at UConn I don’t believe I would have finished. I am so thankful for our friendship, the good times spent together, and the times of grinding out studying for prelims, exams, and our research. Congratulations again on your position at Worcester State, I am looking forward to what we will accomplish together as colleagues right down the road from each other.

To the **many** other graduate students who helped me along the way, thank you. Hyun Chul Jang and Josh Flynn (*BP*) for always dropping everything you were doing to talk some math with me. Bobby Dolan and Noah Hughes for being great friends and office mates. Dan Martin, Phaniel Mariano, and Michelle Rabideau for sharing your insights and experiences to help me get a big head start, you three paved the way for me to be successful. As well



as everyone else my cohort and others, I have many memories of fun times in and outside of the department.

Also, a special shout out to the many friends I met in Connecticut and all of my friends back home in Rhode Island who counted down the years with me. You all always supported me in my drive to go all they way; thank you.

To my parents, Stephen and Linda Miller. Thank you for helping me get through my first five years as an undergrad and then continuing to support me during my Master's degree at RIC. Your love and encouragement undeniably helped me to persevere through the challenges of higher education as well as moving away from home. Your continued support and trips out to Connecticut for football games or just to have dinner made my time extra memorable. I never once felt too far from home.

Finally, I could not have done any other this if it were not for my beautiful wife Lauren. Without any hesitation Lauren picked up her life and moved to Connecticut, the week she graduated, to be with me. I know it was especially challenging being away from your family and friends, a sacrifice you made that I will never forget. At every upturn and downturn, you were there for me. I love you.

# Contents

<b>Ch. 1. Introduction</b>	1
1.1 The Model Problem . . . . .	1
1.2 Notation . . . . .	3
1.3 Basic Results . . . . .	6
<b>Ch. 2. Introduction to Finite Elements</b>	7
2.1 The Continuous Case . . . . .	7
2.2 The Discrete Case . . . . .	10
2.2.1 Triangulation of $\Omega$ . . . . .	10
2.2.2 A Discrete Subspace of Functions. . . . .	12
2.2.3 The Discrete Problem. . . . .	14
2.2.4 Summary on the Advantages to FEM . . . . .	17
<b>Ch. 3. Green's Functions</b>	19
3.1 The Classical Green's Function . . . . .	19
3.2 The Discrete Green's Function . . . . .	22
3.3 A Regularized Green's Function . . . . .	24
3.4 Results on the Regularized Green's Function . . . . .	26
3.5 Results on the Discrete Green's Function . . . . .	33
<b>Ch. 4. On the Positivity of the Discrete Green's Function in 3D</b>	38
4.1 Positivity at the Singularity . . . . .	39
4.2 Positivity away from the Singularity . . . . .	42
<b>Ch. 5. Numerical Results</b>	45
5.1 A Cubic Mesh . . . . .	45
5.2 A Cubic Mesh with Local Refinement . . . . .	50

<b>Ch. 6. Conclusions and Open Problems</b>	52
6.1 Conclusions . . . . .	52
6.2 Open Problems . . . . .	53
<b>Ch. A. Appendices</b>	54
A.1 Miscellaneous Proofs . . . . .	54
A.2 Scott-Zhang Interpolation Operator . . . . .	55
<b>Bibliography</b>	58

# List of Tables

5.1	Discrete Green's function values using uniform refinement. . . . .	48
5.2	Discrete Green's function values using uniform refinement across shortest diagonal. . . . .	49
5.3	Discrete Green's function values using longest edge bisection. . . . .	49
5.4	Discrete Green's function values using local and uniform mesh refinement. . . . .	51
5.5	Discrete Green's function values using local and uniform refinement across shortest diagonal. . . . .	51

# List of Figures

2.1	An example of a two dimensional mesh of a square. $h = \frac{\sqrt{2}}{10}$ . . . . .	11
2.2	An example of a three dimensional mesh of a cube. . . . .	11
2.3	An example of an arbitrary $2D$ basis function. . . . .	13
5.1	First triangulation of the cubic domain. . . . .	46
5.2	Uniform refinement of a single tetrahedron. . . . .	46
5.3	Uniform refinement of a single tetrahedron across shortest diagonal. . . . .	47
5.4	Longest edge bisection refinement of a single tetrahedron. . . . .	48

# Chapter 1

## Introduction

### 1.1 The Model Problem

Let  $\Omega \subset \mathbb{R}^N$ ,  $N = 2, 3$ , be a convex bounded domain with sufficiently smooth boundary. We consider the following Laplace equation:

$$\begin{aligned} -\Delta u &= 0, & \text{in } \Omega \\ u &= b, & \text{on } \partial\Omega. \end{aligned} \tag{1.1}$$

Here we assume the boundary data  $b \in C(\partial\Omega)$  and  $b \geq 0$ .

**Definition 1.1.1.** *A function satisfying (1.1) is called a harmonic function on  $\Omega$ .*

Harmonic functions in the classical sense have been well studied across mathematics, mathematical physics, and stochastic processes. Many results are established for harmonic functions, including; regularity results, Liouville's Theorem, weak and strong maximum principles, as well as a mean value property for example. The maximum principle states if

$\Omega_0$  is a nonempty compact subset of  $\Omega$ , then a harmonic function  $u$  restricted to  $\Omega_0$  attains its maximum and minimum values on the boundary of  $\Omega_0$ . It is an essential tool in the analysis of partial differential equations. Another important and well known result for non-negative harmonic functions is the Harnack inequality [7].

**Theorem 1.1.2** (A. Harnack, 1887). *Assume  $u$  is a non-negative solution to (1.1). Then for any connected open subset  $\Omega_0 \subset\subset \Omega$ , there exists  $C \geq 1$  (depending on  $\Omega_0$ ) such that for any two points  $x, y \in \Omega_0$  we have*

$$u(x) \leq Cu(y).$$

This theorem essentially states that any two values of a non-negative harmonic function are comparable with a constant independent of the particular function itself. The inequality has been useful in the analysis of fully non-linear elliptic problems. This theorem was then extended by Moser in 1961 [12] for uniformly elliptic equations in divergence form with bounded measurable coefficients under the assumption the eigenvalues of the matrix operator are bounded from above and below. Later in 1980, Krylov and Safonov extended the theorem to elliptic equations in non-divergence form with bounded measurable coefficients [9]. In addition there is literature on the Harnack inequality outside of the Euclidean setting on  $\mathbb{R}^N$  including, probability, graph theory, and infinite dimensional operators.

The same cannot be said about the discrete setting, especially when the discretization is less structured. To the author's knowledge there are only two existing papers on the Harnack inequality in the finite element literature. The first is a paper by Aguilera and Caffarelli [1] where they adapted the continuous De Giorgi-Nash-Moser iteration technique. However, this technique required the discrete maximum principle as well as other additional geometric constraints on the discretization. In 2014, Leykekhman and Pruitt established a discrete Harnack inequality [10] on general quasi-uniform meshes in two dimensions only requiring

a mesh condition near the boundary of the domain. Their technique involved using upper and lower bounds on both the continuous Green's function and discrete Green's functions as well as applying analytical tools from Sobolev space theory and finite elements theory. We believe a discrete Harnack Inequality can be used to prove discrete Hölder estimates as well as to analyze the discrete non-linear elliptic problem.

In this thesis we will work towards establishing criteria for the non-negativity of the discrete Green's function with the long term goal of establishing a discrete type Harnack inequality in three dimensions. We will also prove pointwise upper bounds and establish some  $L^p$  estimates for the discrete Green's function. We will adapt techniques used by Leykekhman and Pruitt as well as introduce new analytical techniques while working to keep the discretization of the original space as general as possible. In addition we will provide results of independent interest on a "smooth" Green's function, described in Chapter 3. In three dimensions these results may be used in optimal control problems or results concerning the discrete maximum principle. In chapter 5, we will provide numerical results for the discrete Green's function on polyhedral domains.

## 1.2 Notation

Throughout this thesis we will make use of standard Sobolev notation for which we will provide here and relevant finite element notation will be given in the next chapter.

- We will designate  $C$  as a generic constant that will change throughout the thesis.
- We will employ standard  $L^p$  spaces with associated norms,

$$\|u\|_{L^p(\Omega)} := \left( \int_{\Omega} |u|^p dx \right)^{\frac{1}{p}} < \infty, \text{ for } 1 \leq p < \infty.$$



- We then have the  $L^\infty$  space with associated norm,

$$\|u\|_{L^\infty(\Omega)} := \operatorname{ess\,sup}_\Omega |u|.$$

- We will also occasionally make use of a *multi-index* notation.

- A vector of the form  $\alpha = (\alpha_1, \dots, \alpha_N)$ , where each component  $\alpha_i \in \mathbb{N}$ , is called a *multi-index of order*

$$|\alpha| = \alpha_1 + \dots + \alpha_N.$$

- Given a multi-index  $\alpha$ , we define

$$D^\alpha u(x) := \frac{\partial^{|\alpha|} u(x)}{\partial x_1^{\alpha_1} \dots \partial x_N^{\alpha_N}}.$$

- If  $k$  is a non-negative integer,

$$D^k u(x) := \{D^\alpha u(x) \mid |\alpha| = k\},$$

the set of all partial derivatives of order  $k$ .

- We shall also make use of standard Sobolev spaces and their appropriate norms, that is the space  $W^{k,p}(\Omega)$  and the associated norms,

$$\|u\|_{W^{k,p}(\Omega)} := \left( \sum_{|\alpha| \leq k} \int_\Omega |D^\alpha u| \, dx \right)^{\frac{1}{p}} \text{ for } (1 \leq p < \infty).$$

$$\|u\|_{W^{k,\infty}(\Omega)} := \sum_{|\alpha| \leq k} \operatorname{ess\,sup}_\Omega |D^\alpha u|.$$

- Note: It is customary to write

$$H^k(\Omega) = W^{k,2}(\Omega).$$

- We denote by

$$W_0^{k,p}(\Omega)$$

the closure of  $C_c^\infty(\Omega)$ , of infinitely differentiable functions with compact support, in  $W^{k,p}(\Omega)$ . Thus  $u \in W_0^{k,p}(\Omega)$  if and only if there exist functions  $u_m \in C_c^\infty(\Omega)$  such that  $u_m \rightarrow u$  in  $W^{k,p}(\Omega)$ . We interpret  $W_0^{k,p}(\Omega)$  as comprising of those functions  $u \in W^{k,p}(\Omega)$  such that “ $D^\alpha u = 0$  on  $\partial\Omega$ ” for all  $|\alpha| \leq k - 1$ . See Theorem 2.1.2 for more details.

- Note: It is customary to write

$$H_0^k(\Omega) = W_0^{k,2}(\Omega).$$

- In addition we will also make use of the  $H^1$  semi-norm, that is

$$|u|_{H^1(\Omega)} := \left( \int_{\Omega} |\nabla u|^2 dx \right)^{\frac{1}{2}}.$$

- We will also frequently apply standard  $L^2$  inner product notation, that is

$$(u, v)_{\Omega} := \int_{\Omega} u \cdot v dx.$$

- Any further notation shall be provided when needed.

### 1.3 Basic Results

Throughout our analysis we will make extensive use of the Hölder's inequality. We shall present it here due to its importance. The proof can be found in any standard measure theory text.

**Proposition 1.3.1.** *If  $1 \leq p, q \leq \infty$  and  $p^{-1} + q^{-1} = 1$ , then*

$$\int |fg| \, dx \leq \|f\|_{L^p} \|g\|_{L^q}.$$

Note: if  $p = q = 2$ , then we have the standard Cauchy-Schwarz inequality.

Another useful result is the Poincaré Inequality.

**Proposition 1.3.2.** *There exists a constant  $C < \infty$  such that*

$$\|u\|_{W^{1,p}(\Omega)} \leq C|u|_{W^{1,p}(\Omega)}, \quad \forall u \in W_0^{1,p}(\Omega).$$

# Chapter 2

## Introduction to Finite Elements

### 2.1 The Continuous Case

We first begin with homogeneous Dirichlet problem which is needed for Chapter 3. Let  $\Omega \subset \mathbb{R}^N$ ,  $N = 2, 3$ , be a convex bounded domain with sufficiently smooth boundary. We consider the following Laplace's equation:

$$\begin{aligned} -\Delta u &= f(x), & \text{in } \Omega \\ u &= 0, & \text{on } \partial\Omega, \end{aligned} \tag{2.1}$$

where  $f(x) \in L^2(\Omega)$ . The standard procedure is to multiply through by a test function  $v \in H_0^1(\Omega)$  and then integrate by parts to arrive at the following *variational formulation* of the original problem. Find  $u \in H_0^1(\Omega)$  such that the following equation holds for all  $v \in H_0^1(\Omega)$ ,

$$(\nabla u, \nabla v)_\Omega = (f, v)_\Omega. \tag{2.2}$$

The analysis of elliptic operators in variational form is very rich. For example the Lax-Milgram lemma [6] guarantees the existence of a solution to (2.2). In general given a Hilbert space  $H$  with associated norm  $\|\cdot\|$  and  $a(u, v)$  is a bilinear form on  $H \times H$ . The Lax-Milgram lemma states;

**Lemma 2.1.1** (Lax and Milgram, 1954). *Assume that  $a(u, v) : H \times H \rightarrow \mathbb{R}$  is a bilinear mapping, for which there exists constants  $\alpha, \beta > 0$  such that,*

$$|a(u, v)| \leq \alpha \|u\| \|v\|, \quad \forall u, v \in H, \quad (\text{bounded}),$$

and

$$\beta \|u\|^2 \leq a(u, u) \quad \forall u \in H, \quad (\text{coercive}).$$

Also, let  $(f, v)$  be a continuous linear functional on  $H$ . Then there exists a unique element  $u \in H$  such that,

$$a(u, v) = (f, v),$$

for all  $v \in H$ .

In our case, applying  $a(u, v) = (\nabla u, \nabla v)_\Omega$  and  $(f, v) = (f, v)_\Omega$  we obtain a unique solution to problem (2.2). There are also many results analyzing the regularity of the solutions to elliptic problems in an attempt to gain as much information as possible.

Now in order to define the variational formulation for our modal problem (1.1) with non-homogeneous Dirichlet boundary conditions we need to define the trace of a function  $u \in W^{1,p}(\Omega)$ .

**Theorem 2.1.2.** *Assume  $\Omega$  is bounded and  $\partial\Omega$  is  $C^1$ . Then there exists a bounded linear*

operator

$$T : W^{1,p}(\Omega) \rightarrow L^p(\partial\Omega),$$

such that

$$(i) \quad Tu = u|_{\partial\Omega} \text{ if } u \in W^{1,p} \cap C(\bar{\Omega}) \text{ and}$$

$$(ii) \quad \|Tu\|_{L^p(\partial\Omega)} \leq C\|u\|_{W^{1,p}(\Omega)},$$

for each  $u \in W^{1,p}(\Omega)$ , with the constant  $C$  depending only on  $p$  and  $\Omega$ , but independent of  $u$ .

The proof of Theorem 2.1.2 can be found in Evans [6] on page 272.

**Definition 2.1.3.** We call  $Tu$  the trace of  $u$  on  $\partial\Omega$ .

We are now ready to transform problem (1.1) into the zero boundary condition setting. Suppose  $u \in H^1(\Omega)$  is a weak solution to

$$\begin{aligned} -\Delta u &= 0, & \text{in } \Omega \\ u &= b, & \text{on } \partial\Omega. \end{aligned} \tag{2.3}$$

Here we assume  $b \in C(\partial\Omega)$  and  $b \geq 0$  is the boundary data. This means that  $u = b$  on  $\partial\Omega$  in the trace sense. Therefore we need  $b$  to be the trace of some  $H^1$  function, say  $w$ . Then  $\tilde{u} := u - w$  belongs to  $H_0^1(\Omega)$  and is a weak solution of the boundary value problem

$$\begin{aligned} -\Delta \tilde{u} &= -\Delta w, & \text{in } \Omega \\ \tilde{u} &= 0, & \text{on } \partial\Omega. \end{aligned} \tag{2.4}$$

Thus we can proceed as usual by multiplying through by a test function  $v \in H_0^1(\Omega)$  and integrate by parts to arrive at a variational formulation.

As a rule however, the actual solution to our problem cannot be analytically calculated for arbitrary domains. In terms of physical models in fields such as aero-space engineering, fluids flows, and weather models an approximate solution is desirable. The Finite Element method is a popular choice to derive these approximate solutions.

## 2.2 The Discrete Case

### 2.2.1 Triangulation of $\Omega$ .

We begin first by discretizing our domain  $\Omega$  by subdividing it into non-overlapping cells called *elements*. We will exclusively use triangles in  $2D$  and tetrahedrons in  $3D$ , however, squares or cubes are also popular choices for elements. We will also need the subdivision to be *nonconforming*. That is, the vertices (called *nodes*) of each element may not lie on an edge of an element, otherwise we would have what is called a *hanging node*. We then define the *triangulation* of our domain as the union of all elements in the subdivision, denoted  $\mathcal{T}_h$ . That is,

$$\Omega_h = \bigcup_{\tau_i \in \mathcal{T}_h} \tau_i, \quad (2.5)$$

with  $\Omega_h \subseteq \Omega$ . The parameter  $h$  is called the *mesh parameter* and simply represents the maximum edge length in the triangulation. We will also require the triangulation to be both *shape regular* and *quasi-uniform*.

**Definition 2.2.1.** *A triangulation  $\mathcal{T}_h$  is called shape regular if there exists a constant  $c$  such that,*

$$\max_{\tau \in \mathcal{T}_h} \frac{\text{diam}(\tau)^N}{|\tau|} \leq c. \quad (2.6)$$

We can define a *quasi-uniform* mesh as the following:

**Definition 2.2.2.** A triangulation  $\mathcal{T}_h$  is called quasi-uniform if there exists a constant  $\rho > 0$ , independent of  $\mathcal{T}_h$ , such that for  $\tau \in \mathcal{T}_h$ , we have

$$\frac{\max_{\tau \in \mathcal{T}_h} |\tau|}{\min_{\tau \in \mathcal{T}_h} |\tau|} \leq \rho. \quad (2.7)$$

In two dimensions a quasi-uniform mesh bounds the minimum angle of each triangulation uniformly. However, in three dimensions the minimum dihedral angle is not bounded below. Below is an example of a  $2D$  triangulation of the unit square with the corresponding value of the mesh parameter as well as a  $3D$  triangulation of a cube.

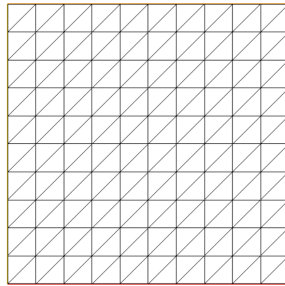


FIGURE 2.1: An example of a two dimensional mesh of a square.  $h = \frac{\sqrt{2}}{10}$ .

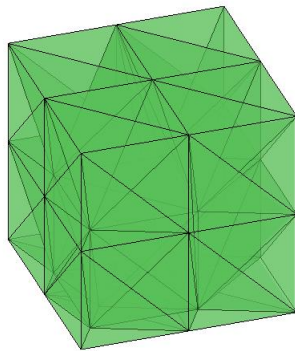


FIGURE 2.2: An example of a three dimensional mesh of a cube.



### 2.2.2 A Discrete Subspace of Functions.

We now wish to interpolate functions from  $H^1(\Omega)$  onto a discrete subspace. As one can imagine there are **many** options to do so. Often the specific choice of functions depends on the problem at hand. For our purposes we shall use continuous, piecewise functions, that are linear when restricted to each element in the triangulation. The choice here is made for a few reasons; we have sufficient regularity of the solutions, the method will be numerically stable, and will be computationally efficient. In addition, the method is positivity preserving. This implies that if the value of the function being interpolated is positive at a node, then it is also positive on the whole element. We will describe what this means now.

We construct the discrete subspace in the following way. Let  $x_i$  for  $i \in \{1, \dots, n\}$  denote interior nodes and  $x_j$  for  $j \in \{n+1, \dots, n+m\}$  denote boundary nodes (those that lie on the boundary). We then define a basis function,  $\phi_k(x)$ , at each node that is equal to one at the respective node and zero at all other nodes. That is,

$$\phi_k(x_l) = \delta_{kl} = \begin{cases} 1, & \text{if } k = l, \\ 0, & \text{if } k \neq l, \end{cases} \quad (2.8)$$

where  $\delta_{kl}$  is the Kronecker delta indicator. Below is an example of a  $2D$  basis function. It should be noted that the support of a basis function is restricted to elements having  $x_i$  as a node.

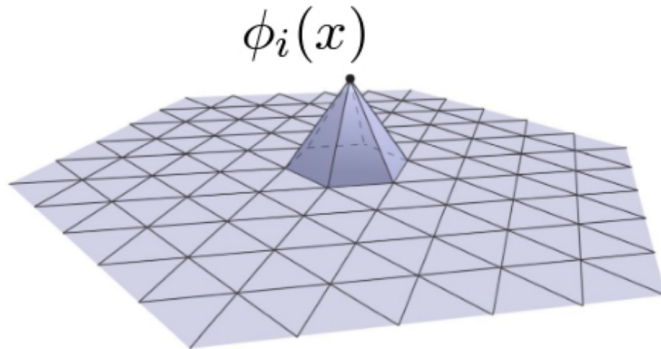


FIGURE 2.3: An example of an arbitrary 2D basis function.

Our discrete subspace will then consist of all finite linear combinations of nodal basis functions. We denote this space by  $V_h(\Omega_h)$  (resp.  $V_h^0(\Omega_h)$  for zero boundary condition) and we note that  $V_h(\Omega_h) \subset H^1(\Omega)$  (resp.  $V_h^0(\Omega_h) \subset H_0^1(\Omega)$ ). We can then define an interpolant for functions from  $H^1(\Omega) \cap C^0(\Omega)$  onto  $V_h(\Omega_h)$ .

**Definition 2.2.3.** *The nodal interpolant of a function  $v(x)$  has the following form;*

$$I_h v := \sum_{i=1}^n v(x_i) \phi_i(x) + \sum_{k=n+1}^{n+m} v(x_k) \phi_k(x), \quad \text{for } x \in \Omega_h. \quad (2.9)$$

**Remark 2.2.4.** *It should be noted here that a function  $u \in H^1(\Omega)$  has no pointwise values in two and three dimensions, hence the nodal interpolant is only valid for  $H^1(\Omega) \cap C^0(\Omega)$ . This can be recovered however by use of the Scott-Zhang Interpolant found in [17]. They make use of an averaging interpolation operator which preserves homogeneous boundary conditions. See appendix section A.2 for details on this operator.*

The abstract definition of a finite element given by Ciarlet which can be found in [3] is as follows:

**Definition 2.2.5.** *Let*

(i)  $\Omega \subseteq \mathbb{R}^N$  be a bounded closed set with nonempty interior and piecewise smooth boundary (the **element domain**),

(ii)  $\mathcal{P}$  be the finite-dimensional space of functions on  $\Omega$  (the space of **shape functions**),  
and

(iii)  $\mathcal{N} = \{x_1, x_2, \dots, x_{n+m}\}$  be a basis for  $\mathcal{P}'$  (the set of **nodal variables**).

Then the triple  $(\Omega, \mathcal{P}, \mathcal{N})$  is called a **finite element**.

### 2.2.3 The Discrete Problem.

Based on the variational formulation (2.2) we can pose the discrete version of the model problem (1.1).

Find  $u_h \in V_h$  to be the solution of the problem,

$$\begin{aligned} (\nabla u_h, \nabla v_h)_{\Omega_h} &= 0, \quad \forall v_h \in V_h^0(\Omega_h), \\ u_h &= I_h b, \quad \text{on } \partial\Omega_h. \end{aligned} \tag{2.10}$$

**Remark 2.2.6.** *We should be careful to note here that  $I_h b$  is a two-dimensional interpolant of the form*

$$I_h b = \sum_{k=n+1}^{n+m} b_k \phi_k,$$

where we sum over boundary basis functions and  $b_k = b(x_k)$ .

**Definition 2.2.7.** *A function  $u_h$  satisfying (2.10) is said to be discrete harmonic on  $\Omega_h$ .*

We now wish to obtain our approximate solution  $u_h$  which requires finding the coefficients  $\alpha_i$  for  $u_h$  expanded using the nodal basis, that is,

$$u_h(x) = \sum_{i=1}^n \alpha_i \phi_i(x) + \sum_{k=n+1}^{n+m} b_k \phi_k(x), \quad (2.11)$$

where the first sum is over the interior nodes and the second sum is over the boundary nodes. Since all basis functions  $\phi_i$  span  $V_h(\Omega_h)$  we have that (2.10) is equivalent to

$$\int_{\Omega_h} \nabla u_h \cdot \nabla \phi_j \, dx = 0, \quad j = 1, \dots, n. \quad (2.12)$$

Substituting the representation for  $u_h$  and we get,

$$\begin{aligned} \int_{\Omega_h} \nabla u_h \cdot \nabla \phi_j \, dx &= \int_{\Omega_h} \nabla \left( \sum_{i=1}^n \alpha_i \phi_i(x) + \sum_{k=n+1}^{n+m} b_k \phi_k(x) \right) \cdot \nabla \phi_j \, dx \\ &= \sum_{i=1}^n \alpha_i \int_{\Omega_h} \nabla \phi_i \cdot \nabla \phi_j \, dx + \sum_{k=n+1}^{n+m} b_k \int_{\Omega_h} \nabla \phi_k \cdot \nabla \phi_j \, dx, \quad j = 1, \dots, n. \end{aligned}$$

We can then interpret the linear system in matrix notation as,

$$A\vec{\alpha} + H\vec{b} = 0. \quad (2.13)$$

The matrix  $A \in \mathbb{R}^{n \times n}$  is the interior *stiffness matrix*, with entries given by  $A_{ij} = (\nabla \phi_i, \nabla \phi_j)_{\Omega_h}$  for  $i, j \in \{1, \dots, n\}$ . The matrix  $H \in \mathbb{R}^{n \times m}$  is the boundary stiffness matrix, with entries given by  $H_{jk} = (\nabla \phi_j, \nabla \phi_k)_{\Omega_h}$  for  $j \in \{1, \dots, n\}$  and  $k \in \{n+1, \dots, n+m\}$ . The vector  $\vec{b}$  contains the boundary data, with  $\vec{b} = (b(x_{n+1}), \dots, b(x_{n+m}))^\top \in \mathbb{R}^m$ . Therefore our solution in matrix form is

$$\vec{\alpha} = -A^{-1}H\vec{b}, \quad (2.14)$$

where  $\vec{\alpha} = (\alpha_1, \dots, \alpha_n)^\top = (u_h(x_1), \dots, u_h(x_n))^\top$  represents the solution at the interior nodes. As a consequence of the Lax-Milgram Lemma 2.1.1 we can see that  $A$  is non-singular. By reinterpreting the matrix multiplication as a sum, we have the representation

$$u_h(x_i) = - \sum_{j=1}^n \sum_{k=1}^m A_{ij}^{-1} H_{jk} b_k. \quad (2.15)$$

An essential consequence of the particular method, commonly referred to as the *Galerkin* method, is **Galerkin Orthogonality**.

**Theorem 2.2.8.** *The finite element solution  $u_h$  solving the Laplace problem (2.1) with homogeneous Dirichlet boundary conditions satisfies the following orthogonality,*

$$(\nabla(u - u_h), \nabla v_h)_{\Omega_h} = 0, \quad \forall v_h \in V_h^0(\Omega_h). \quad (2.16)$$

*Proof.* The theorem is easily realized since the solution  $u$  of (2.1) satisfies the variational formulation (2.2) and that the approximate solution  $u_h$  satisfies the discrete variational formulation  $(\nabla u_h, \nabla v_h)_{\Omega_h} = (f, v_h)_{\Omega_h}$  for all  $v_h \in V_h^0$ . The result follows by subtraction of the two equations and noting that  $V_h^0(\Omega_h) \subset H_0^1(\Omega)$ . □

Galerkin orthogonality is useful in many ways, for example we can prove an a priori best approximation estimate for the approximate solution  $u_h$  in the  $H^1$  norm.

**Theorem 2.2.9.** *The finite element solution  $u_h$  solving the Laplace problem (2.1) with homogeneous Dirichlet boundary conditions satisfies the following best approximation,*

$$\|\nabla(u - u_h)\|_{L^2(\Omega_h)} \leq \|\nabla(u - v_h)\|_{L^2(\Omega_h)}, \quad \forall v_h \in V_h^0(\Omega_h). \quad (2.17)$$

*Proof.* Let  $v_h \in V_h^0(\Omega_h)$  arbitrary and write  $u - u_h = u - v_h + v_h - u_h$ . Then,

$$\begin{aligned}
 \|\nabla(u - u_h)\|_{L^2(\Omega_h)}^2 &= \int_{\Omega_h} |\nabla(u - u_h)|^2 dx \\
 &= \int_{\Omega_h} \nabla(u - u_h) \cdot \nabla(u - v_h + v_h - u_h) dx \\
 &= \int_{\Omega_h} \nabla(u - u_h) \cdot \nabla(u - v_h) + \underbrace{\nabla(u - u_h) \cdot \nabla(v_h - u_h)}_{=0} dx \\
 &\leq \|\nabla(u - u_h)\|_{L^2(\Omega_h)} \|\nabla(u - v_h)\|_{L^2(\Omega_h)},
 \end{aligned}$$

where the Galerkin orthogonality and Cauchy-Schwarz are used. The result follows by dividing through by  $\|\nabla(u - u_h)\|_{L^2(\Omega_h)}$ .

□

**Remark 2.2.10.** *We note here that there are analogues to Theorems 2.2.8 and 2.2.9 for non-homogeneous Dirichlet boundary conditions. However, they are not necessary for our analysis.*

This also shows, using the finite element method, that if  $u$  is well behaved, our discrete solution  $u_h$  is a good approximation in the  $H^1$  norm.

## 2.2.4 Summary on the Advantages to FEM

In order to find our approximate solution,  $u_h$ , we need to solve for  $\vec{\alpha}$ . Notice,  $A$  is a symmetric positive definite matrix which immediately implies existence and uniqueness of the solution. Also, peek back to the picture of the 2D basis function and notice that its support is small. This implies that many of the entries of  $A$  are zero, making it a *sparse* matrix. This is a big computational advantage since it reduces the amount of memory needed for programs like Matlab or FreeFEM to solve a problem. In most cases, the biggest appeal to FEM is the fact

that we can compute approximate solutions that are “close” to the true solutions of PDEs. Fields like engineering, fluid dynamics, and optimal control often desire model solutions or certain qualities of them. Even before any analysis is done we have the following different a priori error estimate of the FEM solution:

$$\|u - u_h\|_{H^1(\Omega)} \leq Ch\|u\|_{H^2(\Omega)}, \quad u_h \in V_h^0(\Omega_h).$$

Since refinements are made on the triangulation and  $h \rightarrow 0$ , we can see that the discrete solution will approach the actual solution weakly.

# Chapter 3

## Green's Functions

Chapter 3 is dedicated to Green's functions. In section 3.1 we will cover some basics on the classical Green's function for the Laplace equation as well as provide necessary estimates. In section 3.2 we will introduce the discrete Green's function. The discrete Green's function is the finite element approximation of the classical Green's function. We will also provide a discrete representation formula for harmonic functions. In section 3.3 we will cover a "smooth" Green's function that will be used throughout the analysis. The remaining two sections will cover analytical results pertaining to the discrete Green's function and the "smooth" Green's function.

### 3.1 The Classical Green's Function

In this section we shall introduce the classical version of the Green's function for the Laplace equation and present some results that are necessary for the analysis of the discrete Green's function. The following can be found in a standard PDE book. In addition, Dr. Sijue Wu's



notes on the Green's function can be found on her webpage.

The Green's function is a tool to solve non-homogeneous linear equations. We can consider a variant of (1.1) with the right hand side equal to  $f(x) \in L^2(\Omega)$ .

$$\begin{aligned} -\Delta u &= f(x), & \text{in } \Omega \\ u &= b, & \text{on } \partial\Omega. \end{aligned} \tag{3.1}$$

One application is  $f$  acting as a heat source and  $u$  represents the current temperature. The idea of a Green's function is that if we know the temperature responding to an impulsive heat source at any point  $z \in \Omega$ . This then allows us to sum up the result with the weight function  $f(z)$  to obtain the temperature responding to the heat source  $f(x) \in \Omega$ . Mathematically we define the Green's function in the following way.

**Definition 3.1.1.** *Define  $G^z(x)$  to be the solution to the following problem;*

$$\begin{aligned} -\Delta G^z(x) &= \delta^z(x), & \text{in } \Omega \\ G^z(x) &= 0, & \text{on } \partial\Omega. \end{aligned} \tag{3.2}$$

*Here  $z \in \Omega$  is a fixed point and  $\delta^z$  is the delta distribution.*

We then have the following:

**Theorem 3.1.2** (Representation formula using Green's function.). *If  $u \in C^2(\bar{\Omega})$  solves problem (3.1), then*

$$u(z) = - \int_{\partial\Omega} b(x) \frac{\partial G^z}{\partial \nu}(x) ds + \int_{\Omega} f(y) G^z(x) dx. \tag{3.3}$$

*Where  $\frac{\partial G^z}{\partial \nu}(y)$  is the outer normal derivative of  $G^z$  with respect to  $x$ .*

Using this theorem, positivity of a harmonic function  $u$  is easily realized. If  $u$  solves problem (1.1), then  $u$  has the following representation,

$$u(x) = - \int_{\partial\Omega} \frac{\partial G^x}{\partial \nu}(y) b(y) d\sigma.$$

It is well known that that Green's function is non-negative, see Lemma 3.1.5, and therefore we must have  $\frac{\partial G^z}{\partial \nu}(y) \leq 0$ . Since the boundary data is non-negative we obtain a non-negative harmonic function.

Another useful property of the Green's function is symmetry of the singularity and function input.

**Theorem 3.1.3.** *For all  $x, z \in \Omega$  with  $x \neq z$  we have*

$$G^z(x) = G^x(z). \tag{3.4}$$

In general, the Green's function is often difficult to construct. Examples exist on domains such as a half-space or a ball. However, for more general domains, we do not have an explicit formula for the Green's function. Nonetheless, using the Green's representation (3.3) as well as estimates for the Green's function, we can obtain further information about solutions to our problem.

We will then require upper and lower bounds on the Green's function. The proof of the following result for general second order elliptic equations can be found in [8].

**Lemma 3.1.4.** *Let  $G^z(x)$  denote the Green's function of the Laplace equation on  $\Omega \subset \mathbb{R}^N$ .*

Then the following estimates hold,

$$|G^z(x)| \leq \begin{cases} C(1 + |\ln |x - z||), & N = 2, \\ C|x - z|^{2-N}, & N \geq 3, \end{cases} \quad (3.5a)$$

$$|\nabla_x^\alpha \nabla_z^\beta G^z(x)| \leq C|x - z|^{2-N-|\alpha|-|\beta|}, \quad |\alpha| + |\beta| \geq 1. \quad (3.5b)$$

There also exists a lower bound for the Green's function which can be found in section 7 of [11].

**Lemma 3.1.5.** *Let  $G^z(x)$  denote the Green's function of the Laplace equation on  $\Omega \subset \mathbb{R}^N$ ,  $N \geq 3$ . Then the following estimate holds for some  $C > 0$ ,*

$$C|x - z|^{2-N} \leq G^z(x). \quad (3.6)$$

We note that when  $N = 3$  we have the following estimates on  $G^z(x)$ ,

$$C_1|x - z|^{-1} \leq G^z(x) \leq C_2|x - z|^{-1}. \quad (3.7)$$

## 3.2 The Discrete Green's Function

In this section we will present the discrete Green's function that arise from the finite element method. This function is simply the finite element approximation of the classical Green's function  $G^z(x)$  and does not have a true singularity associated with it. However, we can define the discrete Green's function in a similar manner.

**Definition 3.2.1.** *The discrete Green's function with singularity at  $z$  is the function  $G_h^z(x) \in$*

$V_h^0(\Omega_h)$  satisfying

$$(\nabla G_h^z, \nabla v_h)_\Omega = v_h(z), \quad \forall v_h \in V_h^0(\Omega_h). \quad (3.8)$$

From this definition it is clear to see that  $G_h^z(x)$  is also symmetric by replacing  $v_h$  with  $G_h^x(z)$ . Next, we shall show the discrete equivalent of the Green's function representation 3.1.2 using the discrete Green's function. This representation can also be found in [5]. First we know that the vector  $\vec{G}^{(i)} = (G_h^{x_i}(x_1), \dots, G_h^{x_i}(x_n))^T$  solves

$$A\vec{G}^{(i)} = \vec{B}^{(i)}, \quad (3.9)$$

where  $A$  is the stiffness matrix defined in section 2.2.3 and  $B_j^{(i)} = (\delta^{x_i}, \phi_j) = \phi_j(x_i) = \delta_{ji}$  (the Kronecker delta indicator). This is due to the definition 3.2.1 of  $G_h^z$ . Therefore if we interpret the vectors as column matrices then we can compactly write the equations as

$$A[\vec{G}^{(1)}, \dots, \vec{G}^{(n)}] = [\vec{B}^{(1)}, \dots, \vec{B}^{(n)}] = \mathcal{I}_n. \quad (3.10)$$

Which shows that

$$G_h^{x_i}(x_j) = (A^{-1})_{ij}. \quad (3.11)$$

In other words, the values of the discrete Green's function at nodal points are the corresponding entries in the inverse of the stiffness matrix  $A$  if we use the nodal basis. Thus from (2.15) we get a discrete Green's representation for discrete Harmonic functions.

**Definition 3.2.2** (Discrete Green's Representation). *If  $u_h \in V_h(\Omega_h)$  solves (2.10), then*

$$u_h(x_i) = - \sum_{j=1}^n \sum_{k=1}^m G_h^{x_i}(x_j) H_{jk} B_k. \quad (3.12)$$

### 3.3 A Regularized Green's Function

In the analysis we will also need a regularized Green's function. To define this we first need a regularized delta function.

**Definition 3.3.1.** Let  $\tilde{\delta}^z(x) \geq 0$  denote a regularized delta function supported in an element  $\tau_0$  containing  $z$  defined by,

$$(\tilde{\delta}^z, v_h)_\Omega = (\tilde{\delta}^z, v_h)_{\tau_0} = v_h(z), \quad \forall v_h \in V_h(\Omega_h). \quad (3.13)$$

For an explicit construction of  $\tilde{\delta}^z$  see [2] or [16]. In addition we also have the following estimates for  $\tilde{\delta}^z$ .

**Lemma 3.3.2.** Let  $\tau_0$  be the element  $\tilde{\delta}^z$  is supported in. Then there exists a constant  $C$  independent of  $z$  such that,

$$\|\tilde{\delta}^z\|_{W_p^s(\tau_0)} \leq Ch^{-s-N(1-\frac{1}{p})}, \quad 1 \leq p \leq \infty, \quad s = 0, 1. \quad (3.14)$$

Therefore we get in particular;  $\|\tilde{\delta}^z\|_{L^1(\Omega)} \leq C$ ,  $\|\tilde{\delta}^z\|_{L^2(\Omega)} \leq Ch^{-\frac{N}{2}}$ , and  $\|\tilde{\delta}^z\|_{L^\infty(\Omega)} \leq Ch^{-N}$ .

**Remark 3.3.3.** Due to the construction of  $\tilde{\delta}^z$  we have  $\tilde{\delta}^z > 0$  which implies  $\int_{\tau_0} \tilde{\delta}^z dx = 1$ . We will use this observation periodically throughout the analysis. See [2].

Additionally, defining the  $L^2$  projection of a function  $u \in L^2(\Omega)$  onto  $V_h(\Omega)$  by,

$$(P_h u, v_h)_\Omega = (u, v_h)_\Omega, \quad \forall v_h \in V_h(\Omega). \quad (3.15)$$

Then it has been shown that the  $L^2$  projection of  $\tilde{\delta}^z$  has exponential decay away from  $z$ .

The following is Lemma 7.2 in [18].

**Lemma 3.3.4.** *Given a quasi-uniform triangulation  $\Omega_h$  there exists a constants  $C$  and  $c$  such that*

$$|P_h \tilde{\delta}^z(x)| \leq Ch^{-N} e^{-\frac{c|x-z|}{h}}. \quad (3.16)$$

Using  $\tilde{\delta}^z$ , we are then able to define a regularized Green's function.

**Definition 3.3.5.** *The regularized Green's function,  $\tilde{G}^z(x)$ , is defined by*

$$\begin{aligned} -\Delta \tilde{G}^z &= \tilde{\delta}^z, & \text{in } \Omega \\ \tilde{G}^z &= 0, & \text{on } \partial\Omega. \end{aligned} \quad (3.17)$$

If we multiply through the first line of (3.17) by a test function  $v_h \in V_h^0$ , integrate by parts, and apply boundary conditions, we get an alternative definition for  $\tilde{G}^z(x)$ ,

$$(\nabla \tilde{G}^z, \nabla v_h)_\Omega = (\tilde{\delta}^z, v_h)_\Omega = v_h(z), \quad \forall v_h \in V_h^0. \quad (3.18)$$

The second equality is due to  $v_h$  is linear affine on each element. It is worth while to note here that  $G_h^z = R_h \tilde{G}^z = R_h G^z$ , where  $R_h u$  is the Ritz projection of a function  $u \in H_0^1(\Omega)$  onto  $V_h^0(\Omega_h)$  defined by

$$(\nabla R_h u, \nabla v_h)_{\Omega_h} = (\nabla u, \nabla v_h)_{\Omega_h}, \quad \forall v_h \in V_h^0(\Omega_h). \quad (3.19)$$

This implies that  $G_h^z(x)$  is the finite element approximation of both  $G^z(x)$  and  $\tilde{G}^z(x)$ .

### 3.4 Results on the Regularized Green's Function

In this section we shall present some results concerning the regularized Green's function. It is important to note that these results are valid for  $N = 3$  only. Some of the results will be used later in our analysis of the discrete Green's function and discrete harmonic functions while others are of independent interest. In each proof  $C$  is used to designate a generic constant that may change from step to step. Our first result involves an upper bound, independent of  $h$ , on the  $L^2$  inner product of  $\tilde{\delta}^z$  and  $\tilde{G}^z$ . The lemma also gives an upper bound for  $\tilde{G}^z$  in  $h$ .

**Lemma 3.4.1.** *There exists a constant  $C$  independent of  $h$  and  $z$  such that*

$$(\tilde{G}^z, \tilde{\delta}^z)_\Omega \leq Ch^{-1}. \quad (3.20)$$

*Proof.* Let  $\tau_0$  be the element such that  $\tilde{\delta}^z$  is supported in. Then by Green's representation we have for  $|x - y| \leq ch$ ,  $c$  small,

$$\begin{aligned} \tilde{G}^z(y) &= \int_{\tau_0} G(y, x) \tilde{\delta}^z(x) dx \leq C_G \int_{\tau_0} |x - y|^{-1} \tilde{\delta}^z(x) dx \\ &\leq C_G \int_{\tau_0} |x - y|^{-1} dx \cdot \|\tilde{\delta}^z\|_{L^\infty(\tau_0)}. \end{aligned}$$

$C_G$  is a constant dependent of  $G^z(x)$ . We have by Lemma 3.3.2 that  $\|\tilde{\delta}^z\|_{L^\infty(\Omega)} \leq Ch^{-3}$ . Now we shall convert to spherical coordinates with  $\rho = |x - y|$  and choose  $c$ , small, such that

$\tau_0 \subset B_{ch}(z)$  to get,

$$\begin{aligned} Ch^{-3} \int_{\tau_0} |x - y|^{-1} dx &\leq Ch^{-3} \int_{B_{ch}(z)} |x - y|^{-1} dx \\ &= Ch^{-3} \int_0^{ch} \rho^{-1} \rho^2 d\rho \\ &\leq Ch^{-1}. \end{aligned}$$

Therefore  $\tilde{G}^z(y) \leq Ch^{-1}$ . Thus,

$$(\tilde{G}^z, \tilde{\delta}^z)_\Omega = \int_{\tau_0} \tilde{G}^z \tilde{\delta}^z dx \leq Ch^{-1} \underbrace{\int_{\tau_0} \tilde{\delta}^z dx}_{=1} = Ch^{-1}.$$

□

The next lemma shows that  $\tilde{G}^z$  cannot be uniformly bounded in  $h$ .

**Lemma 3.4.2.** *There exists a constant  $C$  independent of  $h$  and  $z$  such that*

$$(\tilde{G}^z, \tilde{\delta}^z)_\Omega \geq Ch^{-1}. \quad (3.21)$$

*Proof.* Let  $\tau_0$  be the element such that  $\tilde{\delta}^z$  is supported in. Then by Green's representation, for  $x \in B_z(ch)$ ,  $c$  small,

$$\begin{aligned} \tilde{G}^z(z) &= \int_{\tau_0} G(z, x) \tilde{\delta}^z(x) dx \\ &\geq C_G \int_{\tau_0} |x - z|^{-1} \tilde{\delta}^z(x) dx \\ &\geq C_G h^{-1} \int_{\tau_0} \tilde{\delta}^z(x) dx = C_G h^{-1}. \end{aligned}$$



Therefore we get,

$$(\tilde{G}^z, \tilde{\delta}^z)_\Omega = \int_{\tau_0} \tilde{G}^z \tilde{\delta}^z dx \geq C_G h^{-1} \int_{\tau_0} \tilde{\delta}^z dx = C_G h^{-1}.$$

□

As a result of Lemmas 3.4.1 and 3.4.2 we get the following corollary.

**Corollary 3.4.3.** *There exist constants  $C_1$  and  $C_2$  independent of  $h$  and  $z$  such that for  $x \in B_{ch}(z)$ ,  $c$  small, we have*

$$C_1 h^{-1} \leq \tilde{G}^z(x) \leq C_2 h^{-1}, \quad (3.22)$$

and in particular we see,

$$C_1 h^{-1} \leq \tilde{G}^z(z) \leq C_2 h^{-1}, \quad (3.23)$$

The next lemma concerns an upper bound for  $\nabla \tilde{G}^z$  in the  $L^\infty$  norm.

**Lemma 3.4.4.** *There exists a constant  $C$  independent of  $z$  and  $h$  such that*

$$\|\nabla \tilde{G}^z\|_{L^\infty(\Omega)} \leq C h^{-2}. \quad (3.24)$$

*Proof.* Let  $y \in \Omega_h$ . We shall observe two cases.

**Case 1:** Given  $c > 1$ , small, and  $y \in \Omega_h \setminus B_{ch}(z)$ .

We appeal to Green's function representation (3.3);

$$\begin{aligned}
|\nabla \tilde{G}^z(y)| &= \left| \int_{\tau_0} \nabla_y G(y, x) \tilde{\delta}^z(x) dx \right| \\
&\leq \int_{\tau_0} |\nabla_y G(y, x)| |\tilde{\delta}^z(x)| dx \\
&\leq C \int_{\tau_0} |x - y|^{-2} |\tilde{\delta}^z(x)| dx \\
&\leq Ch^{-2} \|\tilde{\delta}^z\|_{L^1(\Omega_h)}, \quad \text{since } |x - y| > ch, \\
&\leq Ch^{-2}.
\end{aligned}$$

Where the last line follows from Lemma 3.3.2. We shall now proceed to case 2.

**Case 2:** Given  $c > 1$ , small and  $y \in B_{ch}(z)$ .

We again appeal to Green's representation as in case 1 in which we still have,

$$|\nabla \tilde{G}^z(y)| \leq C \int_{\tau_0} |x - y|^{-2} |\tilde{\delta}^z(x)| dx.$$

Now we will apply the  $L^\infty$  estimate from Lemma 3.3.2 and the Hölder's inequality to get,

$$\int_{\tau_0} |x - y|^{-2} |\tilde{\delta}^z(x)| dx \leq Ch^{-3} \int_{\tau_0} |x - y|^{-2} dx.$$

We shall now apply spherical coordinates with  $|x - y| = \rho$  to get,

$$\begin{aligned} Ch^{-3} \int_{\tau_0} |x - y|^{-2} dx &\leq Ch^{-3} \int_{B_{ch}(z)} |x - y|^{-2} dx \\ &= Ch^{-3} \int_0^{ch} \rho^{-2} \rho^2 d\rho \\ &\leq Ch^{-3}h = Ch^{-2}. \end{aligned}$$

Since  $y$  is arbitrary, the result follows. □

In addition we will use Lemma 3.4.1 to show an upper bound  $\nabla \tilde{G}^z$  in the  $L^2$  norm.

**Lemma 3.4.5.** *There exists a constant  $C$  independent of  $h$  and  $z$  such that*

$$\|\nabla \tilde{G}^z\|_{L^2(\Omega_h)} \leq Ch^{-\frac{1}{2}}. \quad (3.25)$$

*Proof.* Observe,

$$\begin{aligned} \|\nabla \tilde{G}^z\|_{L^2(\Omega_h)}^2 &= \int_{\Omega_h} \nabla \tilde{G}^z \cdot \nabla \tilde{G}^z dx \\ &= \int_{\Omega_h} \tilde{G}^z \cdot \tilde{\delta}^z dx, \quad \text{by (3.18),} \\ &\leq Ch^{-1}, \quad \text{by 3.20.} \end{aligned}$$

Therefore the result follows. □

Our next result concerns the  $L^1$  norm of the regularized Green's function which requires a different proof technique. The result may be of independent interest, potentially in showing

best approximation results.

**Lemma 3.4.6.** *There exists a constant  $C$  independent of  $h$  and  $z$  such that*

$$\|\nabla \tilde{G}^z\|_{L^1(\Omega_h)} \leq C. \quad (3.26)$$

*Proof.* We shall proceed using a dyadic decomposition of  $\Omega_h$ . With out loss of generality, assume  $\text{diam}(\Omega_h) \leq 1$ . Then let  $d_j = 2^{-j}$  and

$$\Omega_h = \Omega_* \cup \bigcup_{j=0}^J \Omega_j,$$

where

$$\Omega_* = \{x \in \Omega_h \mid |x - z| \leq Kh\},$$

$$\Omega_j = \{x \in \Omega_h \mid d_{j+1} \leq |x - z| \leq d_j\},$$

with  $K$  possibly chosen later and  $J$  such that  $2^{-J} \leq Kh \leq 2^{-J+1}$ . This then gives

$$\|\nabla \tilde{G}^z\|_{L^1(\Omega_h)} \leq \underbrace{\sum_{j=0}^J \|\nabla \tilde{G}^z\|_{L^1(\Omega_j)}}_{(1)} + \underbrace{\|\nabla \tilde{G}^z\|_{L^1(\Omega_*)}}_{(2)}.$$

We will now estimate (1) and (2) individually. For (1) applying the Hölder's inequality first,

$$\begin{aligned}
\|\nabla \tilde{G}^z\|_{L^1(\Omega_j)} &\leq d_j^3 \|\nabla \tilde{G}^z\|_{L^\infty(\Omega_j)} \\
&\leq d_j^3 \int_{\tau_0} C|x-z|^{-2} |\tilde{\delta}^z| dx \\
&\leq C d_j^3 d_{j+1}^{-2} \int_{\tau_0} |\tilde{\delta}^z| dx \\
&\leq C d_j^3 d_j^{-2} \leq C d_j.
\end{aligned}$$

Where the second line follows from Lemma 3.4.4. Therefore,

$$\sum_{j=0}^J \|\nabla \tilde{G}^z\|_{L^1(\Omega_j)} \leq \sum_{j=0}^J C d_j \leq C.$$

To estimate (2) we again appeal to the Hölder's inequality and Lemma 3.4.4 to get,

$$\begin{aligned}
\|\nabla \tilde{G}^z\|_{L^1(\Omega_*)} &\leq K^3 h^3 \|\nabla \tilde{G}^z\|_{L^\infty(\Omega_*)} \\
&\leq C K^3 h^3 h^{-2} \\
&\leq C h.
\end{aligned}$$

In fact, as  $h \rightarrow 0$ , we see that  $\|\nabla \tilde{G}^z\|_{L^1(\Omega_*)} \rightarrow 0$ .

□

Now, using Lemmas 3.4.4 and 3.4.6, we can apply an interpolation inequality for  $L^p$  norms to derive an estimate for  $\|\nabla \tilde{G}^z\|_{L^p(\Omega_h)}$  when  $1 \leq p \leq \infty$ . The following interpolation inequality can be found in [6].

**Theorem 3.4.7.** *Assume  $1 \leq s \leq p \leq t \leq \infty$  and*

$$\frac{1}{p} = \frac{\theta}{s} + \frac{1-\theta}{t}.$$

Suppose also  $u \in L^s(\Omega) \cap L^t(\Omega)$ , then  $u \in L^p(\Omega)$  and

$$\|u\|_{L^p(\Omega)} \leq \|u\|_{L^s(\Omega)}^\theta \|u\|_{L^t(\Omega)}^{1-\theta}.$$

Now with  $s = 1$  and  $t = \infty$  we get  $\theta = \frac{1}{p}$  and

$$\begin{aligned} \|\nabla \tilde{G}^z\|_{L^p(\Omega_h)} &\leq \|\nabla \tilde{G}^z\|_{L^1(\Omega_h)}^{\frac{1}{p}} \|\nabla \tilde{G}^z\|_{L^\infty(\Omega_h)}^{1-\frac{1}{p}} \\ &\leq Ch^{-2(1-\frac{1}{p})} \\ &= Ch^{\frac{2}{p}-2}. \end{aligned}$$

Thus we get the following corollary.

**Corollary 3.4.8.** *There exists a constant  $C$  independent of  $h$  and  $z$  such that*

$$\|\nabla \tilde{G}^z\|_{L^p(\Omega_h)} \leq Ch^{\frac{2}{p}-2}, \quad \text{for } 1 \leq p \leq \infty. \quad (3.27)$$

### 3.5 Results on the Discrete Green's Function

Using the regularized Green's function we shall now present an estimate for the  $L^\infty$  norm of  $G_h^z$  and then give a resulting corollary.

**Lemma 3.5.1.** *There exists a constant  $C$  independent of  $h$  and  $z$  such that*

$$\|G_h^z\|_{L^\infty(\Omega_h)} \leq Ch^{-1}. \quad (3.28)$$

*Proof.* Since  $G_h^z$  is piecewise continuous and linear we know  $\|G_h^z\|_{L^\infty(\Omega_h)}$  is finite for each triangulation  $\Omega_h$ . Moreover we know the maximum value will occur at  $z$ . We shall show

$G_h^z(z) \leq Ch^{-1}$ . Indeed,

$$\begin{aligned}
G_h^z(z) &= (G_h^z, \tilde{\delta}^z)_{\Omega_h} \\
&= (\nabla G_h^z, \nabla G_h^z)_{\Omega_h} \\
&= \|\nabla \tilde{G}^z\|_{L^2(\Omega_h)}^2 - \|\nabla \tilde{G}^z\|_{L^2(\Omega_h)}^2 + \|\nabla G_h^z\|_{L^2(\Omega_h)}^2 \\
&= (\tilde{G}^z, \tilde{\delta}^z)_{\Omega_h} + \int_{\Omega_h} (|\nabla G_h^z|^2 - |\nabla \tilde{G}^z|^2) dx \\
&= (\tilde{G}^z, \tilde{\delta}^z)_{\Omega_h} - \int_{\Omega_h} (|\nabla \tilde{G}^z|^2 - |\nabla G_h^z|^2) dx \\
&= (\tilde{G}^z, \tilde{\delta}^z)_{\Omega_h} - (\nabla(\tilde{G}^z - G_h^z), \nabla(\tilde{G}^z + G_h^z))_{\Omega_h} \\
&= (\tilde{G}^z, \tilde{\delta}^z)_{\Omega_h} - (\nabla(\tilde{G}^z - G_h^z), \nabla \tilde{G}^z)_{\Omega_h} \\
&= (\tilde{G}^z, \tilde{\delta}^z)_{\Omega_h} - (\nabla(\tilde{G}^z - G_h^z), \nabla(\tilde{G}^z - G_h^z))_{\Omega_h} \\
&= (\tilde{G}^z, \tilde{\delta}^z)_{\Omega_h} - \|\nabla(\tilde{G}^z - G_h^z)\|_{L^2(\Omega_h)}^2 \\
&\leq (\tilde{G}^z, \tilde{\delta}^z)_{\Omega_h} = (\tilde{G}^z, \tilde{\delta}^z)_{\tau_0} \\
&\leq Ch^{-1}.
\end{aligned}$$

We have used the Galerkin orthogonality and Lemma 3.20.

□

We then have a resulting corollary.

**Corollary 3.5.2.** *The  $L^2$  norm of  $\nabla G_h^z$  is bounded above by the  $L^2$  norm of  $\nabla \tilde{G}^z$ , that is*

$$\|\nabla G_h^z\|_{L^2(\Omega_h)} \leq \|\nabla \tilde{G}^z\|_{L^2(\Omega_h)} \leq Ch^{-\frac{1}{2}}. \quad (3.29)$$

*Proof.* This follows from showing

$$\int_{\Omega_h} |\nabla G_h^z|^2 - |\nabla \tilde{G}^z|^2 dx = -\|\nabla(\tilde{G}^z - G_h^z)\|_{L^2(\Omega_h)}^2 \leq 0.$$

□

Next we shall show the discrete Green's functions decays exponentially for values away from the singularity. First we need the following definition.

**Definition 3.5.3.** *The discrete Laplace operator,  $\Delta_h : V_h^0(\Omega_h) \rightarrow V_h^0(\Omega_h)$ , is defined by*

$$(-\Delta_h v_h, \chi)_\Omega = (\nabla v_h, \nabla \chi)_\Omega, \quad \forall \chi \in V_h^0(\Omega_h). \quad (3.30)$$

The discrete Laplace operator is an analog of the continuous Laplace operator defined on a discrete subspace of functions, sometimes referred to as the Laplacian matrix.

**Lemma 3.5.4.** *Let  $\epsilon > 0$  and  $x \in \Omega \setminus B_{h^{1-\epsilon}}(z)$ . Then there exists a constants  $C$  and  $c$  independent of  $z$  and  $h$  such that*

$$G_h^z(x) \leq Ch^{-3} e^{-\frac{c|x-z|}{h}}. \quad (3.31)$$

*Proof.* We shall use the fact that the discrete Laplace operator is bounded as well as estimate (3.16). First note that by (3.8), (3.13), (3.15), and (3.30) we have,

$$-\Delta_h G_h^z = P_h \tilde{\delta}^z. \quad (3.32)$$



Therefore we get,

$$\begin{aligned}
G_h^z(x) &= (\tilde{\delta}^x, G_h^z)_{\tau_x} = (\tilde{\delta}^x, (-\Delta_h)^{-1} P_h \tilde{\delta}^z)_{\tau_x} \\
&\leq C \|\tilde{\delta}^x\|_{L^1(\tau_x)} \|(-\Delta_h)^{-1} P_h \tilde{\delta}^z\|_{L^\infty(\tau_x)} \\
&\leq C \|P_h \tilde{\delta}^z\|_{L^\infty(\tau_x)} \\
&\leq Ch^{-3} e^{-\frac{|x-z|}{h}}.
\end{aligned}$$

□

We first note that this result does not give us insight to the positivity of  $G_h^z(x)$ . However, in contrast to Lemma 3.5.1 we gain a significantly sharper bound on the discrete Green's function for  $x$  outside of a ball around the singularity. This is due to for  $|x-z| \geq ch^{1-\epsilon}$  we have  $e^{-\frac{|x-z|}{h}} \leq C_\epsilon h^{-3}$ . This then implies that the behavior of  $G_h^z(x)$  is most interesting in  $B_z(h^{1-\epsilon})$  for  $\epsilon > 0$ .

Next, we present an upper bound for the discrete Green's function in the  $W_\infty^1(\Omega)$  norm.

**Lemma 3.5.5.** *There exists a constant  $C$  independent of  $h$  such that*

$$\|G_h^z\|_{W_\infty^1(\Omega)} \leq Ch^{-2}. \quad (3.33)$$

*Proof.* We first note that by Theorem 4.5.11 in [3] we have the following,

$$\|G_h^z\|_{W_\infty^1(\Omega)} \leq Ch^{-\frac{3}{2}} \|G_h^z\|_{H^1(\Omega)}.$$

Then since  $G_h^z \in H_0^1(\Omega)$  we have,

$$\|G_h^z\|_{H^1(\Omega)} \leq C |G_h^z|_{H^1(\Omega)}.$$

Therefore applying Corollary 3.5.2 and Lemma 3.4.5 we see,

$$\begin{aligned} Ch^{-\frac{3}{2}}|G_h^z|_{H^1(\Omega)} &\leq Ch^{-\frac{3}{2}}\|\nabla\tilde{G}^z\|_{L^2(\Omega_h)} \\ &\leq Ch^{-\frac{3}{2}}h^{-\frac{1}{2}} \\ &\leq Ch^{-2}, \end{aligned}$$

and we arrive at the desired result. □

This result is most notable close to the singularity as it may suggest, due to Lemma 3.5.1, that the discrete Green's function will have a persistent negative value. Otherwise, this result along with Lemma 3.5.1 can be thought of as an analog to the upper bounds of the continuous elliptic Green's function since this result implies,

$$\|\nabla G_h^z\|_{L^\infty(\Omega)} \leq Ch^{-2}.$$

Additionally, since Corollary 3.5.2 and Lemma 3.5.5 give,

$$\begin{aligned} \|\nabla G_h^z\|_{L^2(\Omega)} &\leq Ch^{-\frac{1}{2}} \quad \text{and} \\ \|\nabla G_h^z\|_{L^\infty(\Omega)} &\leq Ch^{-2}, \end{aligned}$$

we arrive at a similar interpolation inequality for the discrete Green's function.

**Corollary 3.5.6.** *There exists a constant  $C$  independent of  $h$  and  $z$  such that*

$$\|\nabla G_h^z\|_{L^p(\Omega_h)} \leq Ch^{\frac{3}{p}-2}, \quad \text{for } 2 \leq p \leq \infty. \quad (3.34)$$

# Chapter 4

## On the Positivity of the Discrete Green's Function in 3D

It is well known that the classical Green's function for (1.1) is positive. However, the discrete setting is not as straightforward. For  $N = 2$ , Drăgănescu, et al. [5], provided a counterexample showing on general meshes the discrete Green's function may have a persistent negative value. For these meshes, the negative value and the singularity were both an  $O(h)$  away from the boundary of the mesh. In  $N = 2$ , Leykekhman and Pruitt [10], showed on a quasi-uniform, shape regular mesh of a polygonal domain, that if the singularity is of  $O(1)$  away from the boundary the discrete Green's function must eventually be non-negative. With the help of (3.12) they were then able to show the non-negativity of discrete harmonic functions which then led to the establishment of a discrete Harnack type inequality.

In this chapter we will work towards showing the positivity of the discrete Green's function in three dimensions.

## 4.1 Positivity at the Singularity

Positivity at the singularity is a simple consequence of the Definition 3.2.1 of the discrete Green's function. By choosing  $v_h = G_h^z$  we see that,

$$G_h^z(z) = (\nabla G_h^z, \nabla G_h^z)_\Omega = |G_h^z|_{H^1(\Omega)}^2 > 0.$$

Considering estimate (3.7) for the classical Green's function one would expect that  $G_h^z(z) \rightarrow \infty$  as  $h \rightarrow 0$ . In fact, in section 5 of [5], it was conjectured that,

$$G_h^z(z) = O(h^{2-N}) \quad \forall z \text{ (up to the boundary)}.$$

We shall show that this holds for  $N = 3$ , however, the proof can be easily adapted for  $N > 3$ .

**Theorem 4.1.1.** *There exists a constant  $C$  independent of  $h$  and  $z$  such that*

$$G_h^z(z) \geq Ch^{-1}. \tag{4.1}$$

*Proof.* We again note that by (3.8), (3.13), (3.15), and (3.30) we have,

$$-\Delta_h G_h^z = P_h \tilde{\delta}^z, \tag{4.2}$$

where  $-\Delta_h$  is the discrete Laplace operator. Since for all  $v_h \in V_h^0(\Omega_h)$  we have,

$$(-\Delta_h G_h^z, v_h)_\Omega = \underbrace{(\nabla G_h^z, \nabla v_h)_\Omega}_{=v_h(z)} = (\tilde{\delta}^z, v_h)_\Omega = (P_h \tilde{\delta}^z, v_h)_\Omega.$$

Now, for all  $v_h \in V_h^0$  we have by the Poincaré's inequality,

$$C_1(v_h, v_h)_\Omega \leq (\nabla v_h, \nabla v_h)_\Omega = (-\Delta_h v_h, v_h)_\Omega. \quad (4.3)$$

In addition, inverse estimate (4.5.11) in [3] gives,

$$(-\Delta_h v_h, v_h)_\Omega = (\nabla v_h, \nabla v_h)_\Omega \leq C_2 h^{-2} (v_h, v_h)_\Omega. \quad (4.4)$$

Combining (4.3) and (4.4) we see that,

$$C_1 \leq \frac{(v_h, -\Delta_h v_h)_\Omega}{(v_h, v_h)_\Omega} \leq C_2 h^{-2}.$$

This then implies the following estimate which holds by Lemma A.1.1, given in the appendix with proof,

$$C_2^{-1} h^2 \leq \frac{(v_h, (-\Delta_h)^{-1} v_h)_\Omega}{(v_h, v_h)_\Omega} \leq C_1^{-1}. \quad (4.5)$$

Now by (4.2) and (4.5) we have,

$$\begin{aligned} G_h^z(z) &= (\tilde{\delta}^z, G_h^z)_\Omega \\ &= (P_h \tilde{\delta}^z, G_h^z)_\Omega \\ &= (P_h \tilde{\delta}^z, (-\Delta_h)^{-1} P_h \tilde{\delta}^z)_\Omega \\ &\geq C h^2 \|P_h \tilde{\delta}^z\|_{L^2(\Omega)}^2. \end{aligned}$$

Here the key step is to apply the  $L^2$ -projection to  $\tilde{\delta}^z$  in order to project our regularized delta function on  $V_h^0(\Omega)$ .

Therefore it remains to show  $\|P_h \tilde{\delta}^z\|_{L^2(\Omega)}^2 \geq Ch^{-3}$ . Indeed, by (3.15),

$$\|P_h \tilde{\delta}^z\|_{L^2(\Omega)}^2 = (P_h \tilde{\delta}^z, P_h \tilde{\delta}^z)_\Omega = (P_h \tilde{\delta}^z, \tilde{\delta}^z)_\Omega = P_h \tilde{\delta}^z(z),$$

where  $P_h \tilde{\delta}^z(x) = \sum_{i=1}^n \gamma_i \phi_i(x)$  by definition of  $P_h \tilde{\delta}^z \in V_h^0(\Omega_h)$  using the nodal basis. Now for  $z = x_k$ ,  $x_k$  an interior node, we get,  $P_h \tilde{\delta}^{x_k}(x_k) = \sum_{i=1}^n \gamma_i \phi_i(x_k) = \gamma_k$ . In addition, for  $j = 1, \dots, n$  we have,

$$(P_h \tilde{\delta}^{x_k}, \phi_j)_\Omega = (\tilde{\delta}^{x_k}, \phi_j)_\Omega = \phi_j(x_k) = \delta_{kj},$$

and therefore we get,

$$(P_h \tilde{\delta}^{x_k}, \phi_j)_\Omega = \left( \sum_{i=1}^n \gamma_i \phi_i(x), \phi_j \right)_\Omega = \sum_{i=1}^n \gamma_i (\phi_i, \phi_j)_\Omega = \delta_{kj}, \quad j = 1, \dots, n.$$

Interpreting the system as a matrix equation,

$$M \vec{\gamma} = \vec{e}_k,$$

where  $M$  is the *Mass matrix* with entries  $M_{ij} = (\phi_i, \phi_j)_\Omega$ ,  $\vec{\gamma}^\top = (\gamma_1, \dots, \gamma_n)^\top$ , and  $\vec{e}_k^\top = (0, \dots, 0, 1, 0, \dots, 0)^\top$  with 1 in the  $k^{th}$  position. Which then implies,

$$\gamma_k = \vec{e}_k^\top \vec{\gamma} = \vec{e}_k^\top M^{-1} \vec{e}_k. \quad (4.6)$$

Now by properties of the Mass matrix for finite elements in three dimensions, see Rannacher page 121 [13], there exists constants  $c_1$  and  $c_2$  independent of  $h$  such that for any  $\vec{v} \in \mathbb{R}^n \setminus \{\vec{0}\}$ ,

$$c_1 h^3 \leq \frac{\vec{v}^\top M \vec{v}}{\vec{v}^\top \vec{v}} \leq c_2 h^3.$$

Therefore by Lemma A.1.1 we see,

$$c_2^{-1}h^{-3} \leq \frac{\vec{v}^\top M^{-1} \vec{v}}{\vec{v}^\top \vec{v}} \leq c_1^{-1}h^{-3}. \quad (4.7)$$

Thus, choosing  $\vec{v} = \vec{e}_k$  and substituting (4.6) into (4.7) we have shown  $\|P_h \tilde{\delta}^z\|_{L^2(\Omega)}^2 \geq Ch^{-3}$  and the result follows. □

## 4.2 Positivity away from the Singularity

In this section we shall show that the discrete Green's function is positive away from the singularity. The proof technique used will give us insight into the scaling of  $G_h^z$ .

**Lemma 4.2.1.** *Assume for some constant  $K$  that  $|x - z| \geq Kh^{\frac{1}{2}}$ . Then  $G_h^z(x) > 0$ .*

*Proof.* We know using (3.13) that,

$$\begin{aligned} G_h^z(x) &= (G_h^z, \tilde{\delta}^x)_{\tau_x} \\ &= \underbrace{(G_h^z - G^z, \tilde{\delta}^x)_{\tau_x}}_{I_1} + \underbrace{(G^z, \tilde{\delta}^x)_{\tau_x}}_{I_2}, \end{aligned}$$

where  $\tau_x$  is the element containing the support of  $\tilde{\delta}^x$ . Clearly  $I_2$  is positive due to the

properties of  $G^z$  and  $\tilde{\delta}^x$ , however, we can find a lower bound for  $I_2$ . Observe,

$$\begin{aligned}
(G^z, \tilde{\delta}^x)_{\tau_x} &= \int_{\tau_x} G^z(y) \cdot \tilde{\delta}^x(y) dy \\
&\geq C \int_{\tau_x} |x-y|^{-1} \cdot \tilde{\delta}^x(y) dy, \quad \text{by (3.6)} \\
&\geq C(|z-x|+h)^{-1} \int_{\tau_x} \tilde{\delta}^x(y) dy, \quad \text{since } |x-y| \leq ch \\
&\geq C|z-x|^{-1} > 0, \quad \text{by 3.3.3.}
\end{aligned}$$

Now we shall show that  $I_1 \rightarrow 0$  as  $h \rightarrow 0$ , therefore showing  $G_h^z(x) \approx C|z-x|^{-1}$  when  $|x-z| \geq Kh^{\frac{1}{2}}$ , showing that the behavior of  $G_h^z(x)$  is consistent with the classical Green's function. Indeed, we will use Theorem 6.1 in [15] where  $K$  is the constant  $C_7$  in estimate (6.3) which states: if  $|x-z| \geq Kh$ , then

$$|G_h^z(x) - G^z(x)| \leq \frac{Ch^2 \ln\left(\frac{|x-z|}{h}\right)}{|x-z|^3}. \quad (4.8)$$

Adopting the notation  $\omega = \frac{|x-z|}{h}$  and using the assumption (4.8) becomes,

$$\begin{aligned}
|G_h^z(x) - G^z(x)| &\leq \frac{C \ln(\omega)\omega^{-2}}{|x-z|} \\
&\leq \frac{C \ln(\omega)\omega^{-2}}{Kh^{\frac{1}{2}}}.
\end{aligned} \quad (4.9)$$

Additionally  $\omega \geq Kh^{-\frac{1}{2}}$  and observe that  $\ln(\omega)\omega^{-2}$  is decreasing. Therefore it's maximum



must occur at the left endpoint of  $\omega \geq Kh^{-\frac{1}{2}}$  for  $h$  small enough. Now (4.9) becomes,

$$\begin{aligned} |G_h^z(x) - G^z(x)| &\leq \frac{C \ln(\omega)\omega^{-2}}{Kh^{\frac{1}{2}}} \\ &\leq \frac{C \ln(Kh^{-\frac{1}{2}})K^{-2}h}{Kh^{\frac{1}{2}}} \\ &\leq C \ln(Kh^{-\frac{1}{2}})h^{\frac{1}{2}}, \end{aligned}$$

where  $C \ln(Kh^{-\frac{1}{2}})h^{\frac{1}{2}} \rightarrow 0$  as  $h \rightarrow 0$ . Thus,  $G_h^z(x) > 0$ .

□

# Chapter 5

## Numerical Results

In this section we shall provide numerical results concerning the positivity of  $G_h^z(x)$ . The results were obtained using the MATLAB package iFEM [4] developed by Dr. Long Chen at the University of California at Irvine. Some modifications were needed in order to fit our problem as well as to simplify computations. We shall use polygonal domains with the singularity an  $O(1)$  away from the boundary.

### 5.1 A Cubic Mesh

The first mesh we consider is a cube positioned at the nodes  $\{(-1,-1,-1), (-1,-1,1), (-1,1,1), (1,-1,-1), (1,1,-1), (-1,1,-1), (1,-1,1), (1,1,1)\}$  with the singularity at  $z = (-0.75, -0.75, -0.75)$ .

The initial triangulation is Delaunay.

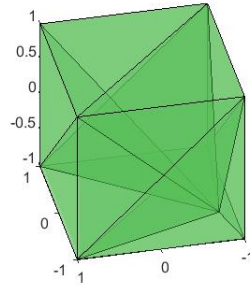


FIGURE 5.1: First triangulation of the cubic domain.

For this mesh we will give two examples using different mesh refinement algorithms. In Table 5.1 a uniform refine is used which subdivides each tetrahedron into 8 smaller and similar “sub-tetrahedrons” of equal volume. This can be done, for example, by adding to the mesh a node at the midpoint of each edge. This will create four tetrahedra in the corners of the original tetrahedron and the remaining four tetrahedra will be constructed from the resulting interior octahedron.

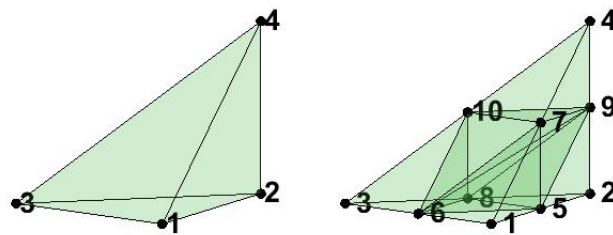


FIGURE 5.2: Uniform refinement of a single tetrahedron.

However through this process we may lose some of the shape regularity of the mesh.

This can be fixed by calculating lengths of the three interior diagonals of the octahedron and subdividing through the shortest diagonal.

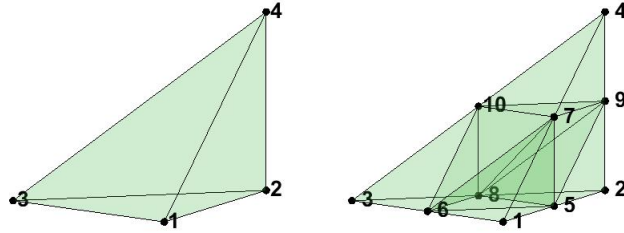


FIGURE 5.3: Uniform refinement of a single tetrahedron across shortest diagonal.

The difference here is subtle. For the interior octahedron, the longest interior diagonal is the line segment between node 6 and node 9. In Figure 5.2 this created the tetrahedron formed by nodes 5, 6, 8, and 9. Once using the shortest interior diagonal, which is the line segment connecting node 7 and node 8, the improved refinement algorithm gives the tetrahedron formed by nodes 5, 7, 8, and 9 instead. The results using this improved algorithm can be seen in Table 5.2. Finally, a third mesh refinement technique is employed. The longest edge of each element in the triangulation is bisected to form a new shape regular and conforming mesh. See Figure 5.4 for an example on a single tetrahedron.

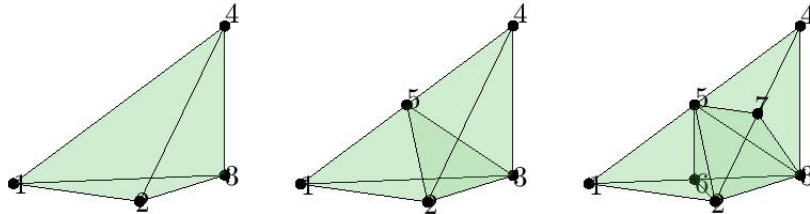


FIGURE 5.4: Longest edge bisection refinement of a single tetrahedron.

Note: In this method, refinement is slow and requires more steps.

No. Nodes	No. Elements	$\min_{x \in \Omega_h} G_h^z(x)$	$\max_{x \in \Omega_h} G_h^z(x)$
35	96	-0.00364467	0.147915
189	768	-0.0148334	0.36481
1241	6144	-0.00754833	0.836731
9009	49152	-0.0038512	1.83258
68705	393216	-0.00141607	3.865363
536769	3.14573e+06	-0.000473936	7.95171

TABLE 5.1: Discrete Green's function values using uniform refinement.

As we can see in Table 5.1 the value of the discrete Green's functions is consistently negative throughout the triangulation refinements.

No. Nodes	No. Elements	$\min_{x \in \Omega_h} G_h^z(x)$	$\max_{x \in \Omega_h} G_h^z(x)$
35	96	-0.00279777	0.148468
189	768	-0.0252328	0.366708
1241	6144	-0.0144661	0.841241
9009	49152	-0.00116218	1.84198
68705	393216	-0.00249823	3.88512
536769	3.14573e+06	-0.000698242	7.99231

TABLE 5.2: Discrete Green's function values using uniform refinement across shortest diagonal.

In Table 5.2, regardless of the improved algorithm we still see a persistent negative values for the discrete Green's function as we further refine the mesh.

No. Nodes	No. Elements	$\min_{x \in \Omega_h} G_h^z(x)$	$\max_{x \in \Omega_h} G_h^z(x)$
16	30	0	0.0553907
25	60	0	0.0940653
44	126	-0.0146393	0.178707
90	312	-0.0071395	0.262382
231	915	-0.0145003	0.453395
699	3073	-0.000705295	0.520141
2404	11299	-0.0152896	0.686233
9804	47555	-0.000907777	1.17272
43099	212468	-0.0150942	1.6141
197433	979772	-3.61518e-05	2.45446

TABLE 5.3: Discrete Green's function values using longest edge bisection.

In Table 5.3 we see again a persistent negative value for the discrete Green's function.

We should note here that the maximum value of the discrete Green's function is not very large. In contrast to Lemma 4.1.1 it may appear as though  $G_h^z(z)$  is scaling incorrectly. However, if we note from the proof of Lemma 4.1.1 we found that  $G_h^z(z) = (\tilde{\delta}^z, G_h^z)_\Omega$ . Since  $(\tilde{\delta}^z, G_h^z)_\Omega = (\tilde{\delta}^z, G_h^z)_{\tau_0}$  we have that the scaling of  $G_h^z(z)$  will depend on the value of  $h$  local to the singularity  $z$ . However, using the uniform refinement algorithm, we see the number of nodes increase by approximately a factor of 8 after the third refinement. In this case, we should see  $G_h^z(z)$  approximately double after each refinement. This is confirmed in the our numerical results. We are now motivated to observe the behavior of the discrete Green's function under a local mesh refinement.

## 5.2 A Cubic Mesh with Local Refinement

For mesh 2, we shall again consider is a cube positioned at the nodes  $\{(-1,-1,-1), (-1,-1,1), (-1,1,1), (1,-1,-1), (1,1,-1), (-1,1,-1), (1,-1,1), (1,1,1)\}$  with the singularity at  $z = (-0.75, -0.75, -0.75)$ . Except we would like to refine locally around the singularity. In this case, we also add in the nodes  $\{(-.74,-.74,-.74), (-.74,-.74,-.76), (-.74,-.76,-.76), (-.76,-.74,-.76), (-.76,-.76,-.74), (-.74,-.76,-.74), (-.76,-.74,-.74), (-.76,-.76,-.76)\}$  to generate the initial mesh. Since each uniform refinement algorithms subdivide each tetrahedra into eight more tetrahedrons, therefore the value of  $h$  will be significantly smaller close to  $z$ . We will present both uniform mesh refinement algorithms from Section 5.1 (uniform refinement and uniform refinement along shortest diagonal).

No. Nodes	No. Elements	$\min_{x \in \Omega_h} G_h^z(x)$	$\max_{x \in \Omega_h} G_h^z(x)$
87	384	0	25
581	3072	-0.000456359	58.5829
4329	24576	-0.14307895	129.212
33617	196608	-0.03656153	272.192
265377	1.57286e+06	-0.0173364	563.858
2.10976e+06	1.25829e+07	-0.0214638	1133.72

TABLE 5.4: Discrete Green's function values using local and uniform mesh refinement.

No. Nodes	No. Elements	$\min_{x \in \Omega_h} G_h^z(x)$	$\max_{x \in \Omega_h} G_h^z(x)$
87	384	0	25
581	3072	-0.000515941	58.7273
4329	24576	-0.00000412	130.022
33617	196608	-0.00275881	273.436
265377	1.57286e+06	-0.00138705	566.92
2.10976e+06	1.25829e+07	-0.00102935	1139.63

TABLE 5.5: Discrete Green's function values using local and uniform refinement across shortest diagonal.

As expected with local mesh refinement, the values of the discrete Green's function are much larger due to the smaller local mesh parameter. In addition, we also observe a persistent negative value.



# Chapter 6

## Conclusions and Open Problems

### 6.1 Conclusions

In this thesis we have established some sharp pointwise bounds on the discrete Green's function. In particular we showed that in three dimensions the discrete Green's function cannot be uniformly bounded in  $h$  at the singularity. Furthermore, we show that away from the singularity the discrete Green's function is positive and decays exponentially to the boundary. We also prove analogous results for the discrete Green's function showing similarities to the continuous Green's function. Numerically, we show that on an a convex domain with sufficiently smooth boundary on an unstructured mesh the discrete Green's function has a persistent negative value.

Additionally we establish  $L^p$  estimates for the gradient of both the discrete and regularized Green's function for  $2 \leq p \leq \infty$ . Furthermore we prove a  $L^1$  estimate for  $\nabla \tilde{G}^z$ . At this time we suspect a similar result can be shown for  $G_h^z$ . Furthermore, establishing a lower bound for  $\nabla G_h^z$  close to the singularity is an immediate priority. We believe these results

could be used in establishing best approximation results in optimal control problems.

## 6.2 Open Problems

Going forward our goal is to theoretically establish the existence of a persistent negative value for the discrete Green's function in three dimensions on unstructured meshes. We also want to investigate under which conditions would guarantee positivity in order to establish a discrete Harnack inequality for discrete Harmonic functions. On two dimensional non-orientable surfaces we would like to establish positivity of the discrete Green's functions and establish a discrete Harnack inequality. Finally, another direction for investigation may include the extension of the Harnack inequality to the inhomogeneous case and to parabolic or more general elliptic equations on non-smooth domains.

# Appendix A

## Appendices

### A.1 Miscellaneous Proofs

In the paper *Variational Bounds on the Entries of a Inverse Matrix* [14] the authors conclude the following result, which was critical in the proof of Lemma 4.1.1 so we felt as though it were important to include a proof of the result.

**Lemma A.1.1.** *Assume  $\vec{v} \in \mathbb{R}^n \setminus \{\vec{0}\}$  and the matrix  $A$  is symmetric. Then if one of the following inequalities holds, the other is equivalent.*

$$\beta \leq \frac{\vec{v}^\top A \vec{v}}{\vec{v}^\top \vec{v}} \leq \alpha \iff \frac{1}{\alpha} \leq \frac{\vec{v}^\top A^{-1} \vec{v}}{\vec{v}^\top \vec{v}} \leq \frac{1}{\beta}. \quad (\text{A.1})$$

*Proof.* We shall start with the left hand result and show it is equivalent to the right hand side. The reverse implication follows immediately. That is, assume

$$\beta \leq \frac{\vec{v}^\top A \vec{v}}{\vec{v}^\top \vec{v}} \leq \alpha,$$

holds for all  $\vec{v} \in \mathbb{R}^n \setminus \{\vec{0}\}$ . Then the result also holds for  $A^{-\frac{1}{2}}\vec{v}$ . Therefore by the symmetry of  $A$  we have,

$$\begin{aligned}
\beta \leq \frac{(A^{-\frac{1}{2}}\vec{v})^\top AA^{-\frac{1}{2}}\vec{v}}{(A^{-\frac{1}{2}}\vec{v})^\top A^{-\frac{1}{2}}\vec{v}} \leq \alpha &\implies \beta \leq \frac{\vec{v}^\top A^{-\frac{1}{2}}A^{\frac{1}{2}}\vec{v}}{(A^{-\frac{1}{2}}\vec{v})^\top A^{-\frac{1}{2}}\vec{v}} \leq \alpha \\
&\implies \beta \leq \frac{\vec{v}^\top A^{-\frac{1}{2}}A^{\frac{1}{2}}\vec{v}}{\vec{v}^\top A^{-\frac{1}{2}}A^{-\frac{1}{2}}\vec{v}} \leq \alpha \\
&\implies \beta \leq \frac{\vec{v}^\top \vec{v}}{\vec{v}^\top A^{-1}\vec{v}} \leq \alpha \\
&\implies \frac{1}{\alpha} \leq \frac{\vec{v}^\top A^{-1}\vec{v}}{\vec{v}^\top \vec{v}} \leq \frac{1}{\beta}.
\end{aligned}$$

□

## A.2 Scott-Zhang Interpolation Operator

In this section we shall give some detail to the Scott-Zhang interpolation operator described in [17]. Recall definition 2.2.5 for a finite element space,

**Definition A.2.1.** *Let*

(i)  $\Omega \subseteq \mathbb{R}^N$  be a bounded closed set with nonempty interior and piecewise smooth boundary (the **element domain**),

(ii)  $\mathcal{P}$  be the finite-dimensional space of functions on  $\Omega$  (the space of **shape functions**),  
and

(iii)  $\mathcal{N} = \{x_1, x_2, \dots, x_{n+m}\}$  be a basis for  $\mathcal{P}$  (the set of **nodal variables**).

Then the triple  $(\Omega, \mathcal{P}, \mathcal{N})$  is called a **finite element**.

The interpolation operator uses an averaging integral over elements or element faces. Our first step is to determine which elements or element faces to restrict our attention to. For any nodal point  $x_i$  we choose an element or an element face  $\sigma_i$  in the following way:

1. If  $x_i$  is an interior point of an element  $\tau$  then,

$$\sigma_i = \tau. \tag{A.2}$$

2. If  $x_i$  is an interior point of a face  $\tau'$  then,

$$\sigma_i = \tau'. \tag{A.3}$$

3. The rest of  $x_i$  will lie on the edge of some element, then we may pick any  $\tau'$  such that  $x_i \in \bar{\tau}'$  subject to the following restriction. If  $x_i \in \partial\Omega_h$  then we must have,

$$\sigma_i = \tau' \quad \text{such that} \quad \tau' \subset \partial\Omega_h. \tag{A.4}$$

We note here that for conforming finite elements  $x_i$  will not fall into cases (1) and (2).

Now, for the nodal basis  $\{\phi_{i,j}\}_{j=1}^{n_0}$  for  $\sigma_i$ , we have a  $L^2(\sigma_i)$ -dual basis  $\{\omega_{i,j}\}$ ,

$$\int_{\sigma_i} \omega_{i,j}(x) \phi_{i,k}(x) dx = \delta_{jk}, \quad j, k = 1, 2, \dots, n_0. \tag{A.5}$$

For simplicity we shall assume that our function is being interpolated at every node  $x_i \in \Omega_h$  therefore equation (A.5) is,

$$\int_{\sigma_i} \omega_i(x) \phi_j(x) dx = \delta_{ij}, \quad i, j = 1, \dots, N. \tag{A.6}$$

Then we have the following interpolation operator.

**Definition A.2.2.** *The Scott-Zhang operator  $\Pi : W^{l,p}(\Omega) \rightarrow V_h(\Omega_h)$  is given by,*

$$\Pi v(x) = \sum_{i=1}^N \phi_i(x) \int_{\sigma_i} \omega_i(y) v(y) dy, \quad (\text{A.7})$$

where  $l \geq 1$  if  $p = 1$  and  $l \geq p^{-1}$  otherwise.

The conditions on  $l$  guarantee that the nodal values,  $\Pi v(x_i)$ , are well defined due to the trace theorem 2.1.2 as well as preserving the validity of homogeneous boundary conditions and the choice of  $\sigma_i$  in (3) preserves the mapping  $\Pi : W_0^{l,p}(\Omega) \rightarrow V_h^0(\Omega_h)$ . Finally, equation (A.6) shows that

$$\int_{\sigma_i} \phi_i(x) v_h(x) dx = v_h(x_i),$$

and we see that  $\Pi$  is a projection such that,

$$\Pi v_h = v_h \quad \forall v \in V_h. \quad (\text{A.8})$$

# Bibliography

- [1] N. E. AGUILERA AND L. A. CAFFARELLI, *Regularity results for discrete solutions of second order elliptic problems in the finite element method*, *Calcolo*, 23 (1986), pp. 327–353 (1987).
- [2] S. BERTOLUZZA, A. DECOENE, L. LACOUTURE, AND S. MARTIN, *Local error estimates of the finite element method for an elliptic problem with a Dirac source term*, *Numer. Methods Partial Differential Equations*, 34 (2018), pp. 97–120.
- [3] S. C. BRENNER AND L. R. SCOTT, *The mathematical theory of finite element methods*, vol. 15 of Texts in Applied Mathematics, Springer, New York, third ed., 2008.
- [4] L. CHEN, *ifem: An integrated finite element method package in matlab*, 2009.
- [5] A. DRĂGĂNESCU, T. F. DUPONT, AND L. R. SCOTT, *Failure of the discrete maximum principle for an elliptic finite element problem*, *Math. Comp.*, 74 (2005), pp. 1–23.
- [6] L. C. EVANS, *Partial differential equations*, vol. 19 of Graduate Studies in Mathematics, American Mathematical Society, Providence, RI, second ed., 2010.
- [7] A. HARNACK, *Über die mit Ecken behafteten Schwingungen gespannter Saiten*, *Math. Ann.*, 29 (1887), pp. 486–499.

- [8] J. P. KRASOVSKĚ, *Properties of Green's functions and generalized solutions of elliptic boundary value problems*, Izv. Akad. Nauk SSSR Ser. Mat., 33 (1969), pp. 109–137.
- [9] N. V. KRYLOV AND M. V. SAFONOV, *A property of the solutions of parabolic equations with measurable coefficients*, Izv. Akad. Nauk SSSR Ser. Mat., 44 (1980), pp. 161–175, 239.
- [10] D. LEYKEKHMAN AND M. PRUITT, *On the positivity of discrete harmonic functions and the discrete Harnack inequality for piecewise linear finite elements*, Math. Comp., 86 (2017), pp. 1127–1145.
- [11] W. LITTMAN, G. STAMPACCHIA, AND H. F. WEINBERGER, *Regular points for elliptic equations with discontinuous coefficients*, Ann. Scuola Norm. Sup. Pisa Cl. Sci. (3), 17 (1963), pp. 43–77.
- [12] J. MOSER, *On Harnack's theorem for elliptic differential equations*, Comm. Pure Appl. Math., 14 (1961), pp. 577–591.
- [13] R. RANNACHER, *Numerische Mathematik 2 (Numerik Partieller Differentialgleichungen)*, 2008.
- [14] P. D. ROBINSON AND A. J. WATHEN, *Variational bounds on the entries of the inverse of a matrix*, IMA J. Numer. Anal., 12 (1992), pp. 463–486.
- [15] A. H. SCHATZ AND L. B. WAHLBIN, *Interior maximum norm estimates for finite element methods*, Math. Comp., 31 (1977), pp. 414–442.
- [16] —, *Interior maximum-norm estimates for finite element methods. II*, Math. Comp., 64 (1995), pp. 907–928.



- [17] L. R. SCOTT AND S. ZHANG, *Finite element interpolation of nonsmooth functions satisfying boundary conditions*, Math. Comp., 54 (1990), pp. 483–493.
- [18] L. B. WAHLBIN, *Local behavior in finite element methods*, in Handbook of numerical analysis, Vol. II, Handb. Numer. Anal., II, North-Holland, Amsterdam, 1991, pp. 353–522.